



Effect of Ni Addition on Bainite Transformation and Properties in a 2000 MPa Grade Ultrahigh Strength Bainitic Steel

Junyu Tian¹ · Guang Xu¹ · Zhengyi Jiang² · Haijiang Hu¹ · Mingxing Zhou^{1,3}

Received: 20 February 2018 / Accepted: 29 April 2018 / Published online: 17 May 2018
© The Korean Institute of Metals and Materials 2018

Abstract

The effects of Nickel (Ni) addition on bainitic transformation and property of ultrahigh strength bainitic steels are investigated by three austempering processes. The results indicate that Ni addition hinders the isothermal bainite transformation kinetics, and decreases the volume fraction of bainite due to the decrease of chemical driving force for nucleation and growth of bainite transformation. Moreover, the product of tensile strength and total elongation (PSE) of high carbon bainitic steels decreases with Ni addition at higher austempering temperatures (220 and 250 °C), while it shows no significant difference at lower austempering temperature (200 °C). For the same steel (Ni-free or Ni-added steel), the amounts of bainite and RA firstly increase and then decrease with the increase of the austempering temperature, resulting in the highest PSE in the sample austempered at temperature of 220 °C. In addition, the effects of austempering time on bainite amount and property of high carbon bainitic steels are also analyzed. It indicates that in a given transformation time range of 30 h, more volume of bainite and better mechanical property in high carbon bainitic steels can be obtained by increasing the isothermal transformation time.

Keywords Nickel · Bainite transformation · Austempering process · Transformation time · Property

Abbreviations

RA	Retained austenite
B _s	Bainite starting temperature
M _s	Martensite starting temperature
Ac ₃	Austenitization finishing temperature during heating
SEM	Scanning electron microscope
XRD	X-ray diffraction
M/A	Martensite/austenite island
YS	Yield strength
TS	Tensile strength
TE	Total elongation

PSE	Product of the tensile strength and total elongation
CCT	Continuous cooling transformation
TTT	Time–temperature–transformation
TRIP	Transformation induced plasticity

1 Introduction

With the great demand on high performance of steel materials, it is necessary to develop new ultrahigh strength steels. Recently, bainitic steels have been a hot topic since it has a potential to satisfy the ever-increasing demands of advanced materials with ultrahigh strength and adequate toughness [1–3]. Ultrahigh strength bainitic steels have various applications such as in vehicles, ships and mechanical engineering [4, 5].

Nickel (Ni), as an important and valuable alloying element, is commonly added in steels. The addition of alloying elements in steels influences not only the transformation behavior, but also the microstructure and properties of steels [6, 7]. Therefore, there is a continuous interest in the effects of alloying elements including Ni on the microstructure and property of steels. Keehan et al. [8] investigated the effects of the addition of Ni (about 4.4 wt%) on microstructure and mechanical

✉ Guang Xu
xuguang@wust.edu.cn

¹ The State Key Laboratory of Refractories and Metallurgy, Hubei Collaborative Innovation Center for Advanced Steels, Wuhan University of Science and Technology, Wuhan 430081, China

² School of Mechanical, Materials, Mechatronic and Biomedical Engineering, University of Wollongong, Wollongong 2522, Australia

³ School of Mechanical and Automotive Engineering, Nanyang Institute of Technology, Nanyang 473004, China

property in high strength weld metals. They reported that the addition of Ni improves hardenability and increases ductility and fracture toughness. Moreover, high percentage of Ni and a few percentage of Ti (0.055 wt%) lead to precipitation of Ni₃Ti which imparts additional hardening [9]. Similarly, Omotoyinbo et al. [10] stated that ultrahigh strength can be obtained by solution and precipitation strengthening due to the addition of high amount of Ni (4.40 wt%) in an austenitic steel. In addition, Zhang et al. [11] reported that Ni addition (4.0 wt%) lowers the transformation temperature of austenite and increases the resistance to brittle fracture of steels at low temperatures in a martensitic stainless steel.

So far, only a few studies discussed the effect of Ni on bainitic transformation in high strength bainitic steels. Chen and Chang [12] elucidated that Ni addition can effectively delay ferrite transformation, decreases martensite starting temperature (M_S) and enlarges the zone of medium-temperature bainite transformation during continuous cooling process. However, the effect of Ni addition on isothermal bainitic transformation, which is an important process to produce the ultrahigh strength bainitic steels, is rarely reported. Therefore, it is worthwhile to further investigate the effects of Ni addition on bainitic transformation, microstructure and property of high carbon bainitic steels treated by austempering process.

In the present study, two kinds of high carbon bainitic steels, with Ni and without Ni addition, and three different austempering processes are designed. The objective is to study the effects of Ni addition on bainitic transformation, microstructure and property in an ultrahigh strength high-carbon bainitic steel. The obtained results are useful to the optimization of the chemical composition and heat treatment process of high carbon bainitic steels.

2 Materials and Experimental

2.1 Materials

The two tested steels were refined using a 50 kg laboratory-scale vacuum furnace followed by hot-rolled and then air-cooled to room temperature. The chemical compositions of two tested steels are presented in Table 1. A high carbon content of the tested steel (0.80 wt%) is to achieve the ultrahigh strength. Manganese (Mn) and chromium (Cr) are added to enhance the stability and hardenability of austenite [13, 14]. Molybdenum (Mo) can improve temper-embrittlement phenomena caused by inevitable impurities [1]. Carbide precipitation is detrimental to the comprehensive properties of steels,

so high percentage of silicon (Si) (1.6 wt%) is added to hinder the formation of carbide [15, 16]. Moreover, high amounts of aluminum (Al) and cobalt (Co) can accelerate the kinetics of bainite transformation and shorten the transformation time [17]. Ni addition in Ni-added steel is to investigate the effect of Ni on bainite transformation, microstructure and property of ultrahigh strength bainitic steels.

2.2 Methods

The bainite starting temperature (B_S) and M_S of two tested steels were calculated to be 347 and 159 °C for Ni-free steel, and 324 and 126 °C for Ni-added steel, respectively, using the software of MUCG83 [18]. Hence, the isothermal temperatures of 200, 220, and 250 °C were chosen for bainite transformation. According to Eq. (1) proposed by Andrews formula [19], the Ac_3 (°C) temperatures were calculated to be 809 and 794 °C for Ni-free steel and Ni-added steel, respectively.

$$Ac_3 = 910 - 203\sqrt{x_c} - 15.2x_{Ni} + 44.7x_{Si} + 104x_v + 31.5x_{Mo} + 13.1x_w \quad (1)$$

where x_i is the mass percent of element “ i ”. Hence, the austenitizing temperature of 900 °C is larger than the corresponding Ac_3 temperature.

Figure 1a shows the continuous cooling transformation (CCT) curves of the two steels calculated by the software of JMatPro7.0 [20]. The detailed experimental procedures are shown in Fig. 1b. After being machined to 140×50×15 mm (L×B×H) blocky samples from steel ingots, they were heated to 900 °C and kept for 30 min for austenite homogenization in a vacuum furnace. The samples after austenitization were rapidly quenched in salt bath furnaces with different temperatures of 200, 220 and 250 °C, respectively, to avoid the high temperature transformation. The austempered samples were taken out from the salt bath furnace after being held for different times of 15, 25 and 30 h, respectively, followed by air-cooled to room temperature.

2.3 Examinations

After the heated treatment, the samples were polished and etched with a 4% nital for microstructure examination. The etched microstructure and fracture morphology were observed by a Nova 400 Nano field emission scanning electron microscope (FE-SEM). The volume fractions of bainite were

Table 1 The chemical compositions of two tested steels (wt%)

Steels	C	Si	Mn	Mo	Cr	Ni	Co	Al
Ni-free	0.803	1.602	1.985	0.303	1.021	–	1.504	0.992
Ni-added	0.799	1.611	2.002	0.301	1.013	1.003	1.502	0.987

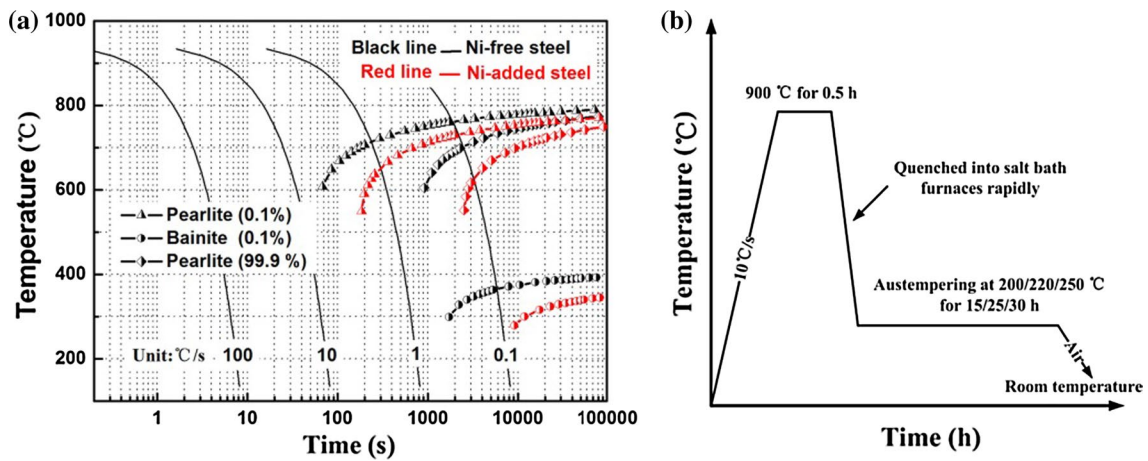


Fig. 1 **a** The continuous cooling transformation (CCT) curves of the two steels; **b** the experimental procedure

counted by the Image-Pro Plus software (Media Cybernetics, Rockville, MD, USA) [21, 22]. To clearly distinguish different phases, the micrographs of 5000 \times magnification were selected. The micrograph of Ni-added steel austempered at 220 °C for 30 h is given in Fig. 2 as an example to show how to calculate the volume fraction of bainite. The microstructure in

this sample consists of bainite, RA and M/A. The darker areas consist of bainite and a small amount of M/A (Fig. 2a). In these darker areas, the bainite is mainly lath-like, and the M/A is blocky. First, the darker areas were automatically colored pink by the software of Image-Pro Plus as shown in Fig. 2b. The area percentage of the pink areas was automatically calculated

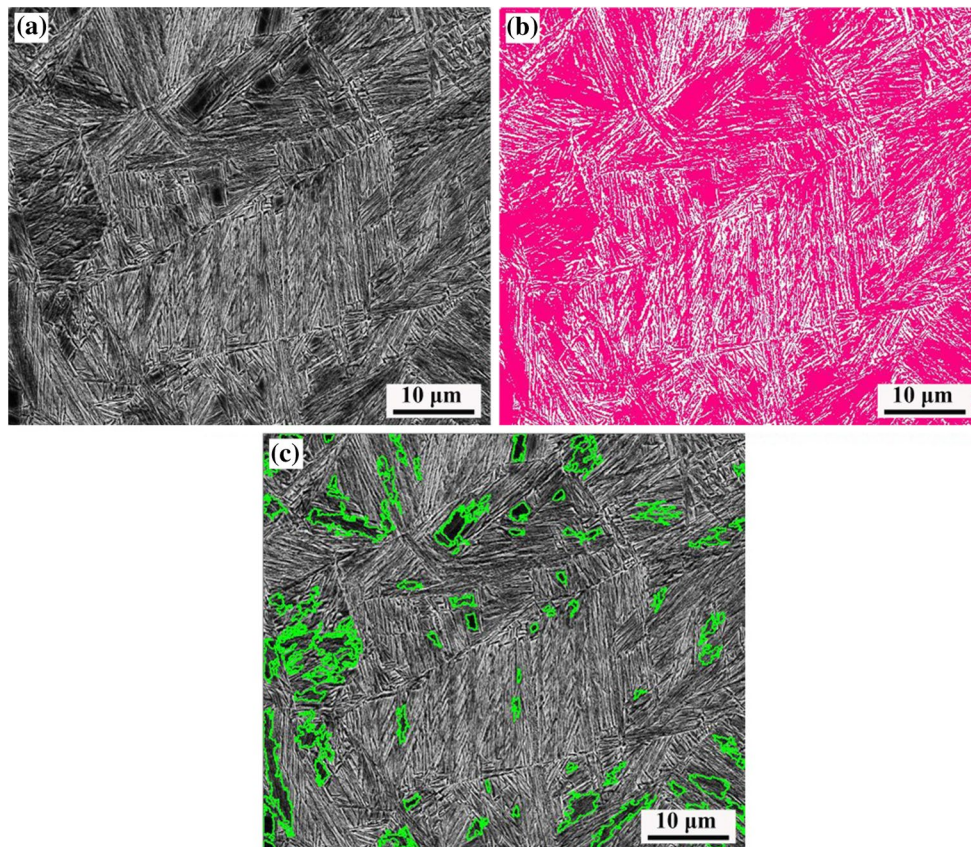


Fig. 2 The example to show how to calculate the volume fraction of bainite: **a** the original micrograph; **b** the darker areas in **a** are colored pink; **c** the darker blocky places are manually marked

by the software, and the result was labeled as A_1 . Second, the darker blocky areas were M/A which were included in A_1 and must be subtracted. The darker blocky areas were carefully and manually marked (Fig. 2c). The area percentage of these areas (labeled as A_2) was measured by the software. Finally, the area percentage of bainite (labeled as A_3) was obtained by $A_3 = A_1 - A_2$. In this example, A_1 was 65.2% and A_2 was 12.9%, so that A_3 was 52.3%. Therefore, the volume fraction of bainite in Fig. 2a was measured to be 52.3%. In order to improve the accuracy of statistical results, six typical SEM photographs with different magnifications were used for each sample, and the average value was reported in the present study. Similarly, other samples of Ni-free and Ni-added steels treated by different procedures could be determined in the same way.

In addition, tensile specimens were prepared according to ASTM standard and conducted at room temperature on an Instron-5969 electronic universal tensile machine at a strain rate of 10^{-3} s^{-1} . The tensile direction was along the rolling direction of steels. In order to obtain the accurate tensile results, three tensile tests were conducted for each sample and the corresponding averages were reported in the present study. The amount of retained austenite (RA) was determined by X-ray diffraction (XRD) experiments on an Empyrean diffractometer, using filtered Co K α radiation and operating at 35 kV and 50 mA.

3 Results and Discussion

3.1 Effect of Ni Addition

3.1.1 Microstructures

The typical microstructures of Ni-free and Ni-added steels after austempering are shown in Fig. 3. Figure 3a, c, e present the microstructures of Ni-free steel austempered at 200, 220 and 250 °C for 30 h, while Fig. 3b, d, f show the microstructures of Ni-added steel austempered at 200, 220 and 250 °C for 30 h, respectively. The microstructures of different samples contains lath-like bainite, blocky martensite/austenite island (M/A) and film-like RA. The volume fractions of bainite were calculated by the Image-Pro Plus software (Media Cybernetics, Rockville, MD, USA) based on the morphology and grayscale of bainite using the method proposed in Sect. 2.3. For the accuracy of the counting results, the total six SEM photographs with different magnifications were used to calculate the bainite amount for each sample. The calculated average values are given in Table 2. It can be observed that when the samples are treated at the same austempering temperature, compared to Ni-free steel, there is less volume of bainite transformation in Ni-added

steel. It indicates that Ni addition retards bainitic transformation and leads to less volume of bainite.

Figure 4a shows the time–temperature–transformation (TTT) curves of two steels calculated by the software of JMatPro 7.0. The TTT curves move to right with Ni addition, indicating that Ni addition increases the incubation period of bainite transformation and prolongs the completing time of bainite transformation, i.e., the kinetics of bainite transformation is hindered by Ni addition. The main reason is that Ni is an austenite stabilizing element. Ni addition lowers the difference of the free energy between γ and α , and decreases the driving force of the transformation from γ to α ($\Delta G^{\gamma \rightarrow \alpha}$). Figure 4b gives the results of $\Delta G^{\gamma \rightarrow \alpha}$ calculated by the software of MUCG83. It shows that the $\Delta G^{\gamma \rightarrow \alpha}$ decreases with Ni addition from -1175 to -1057 J/mol at 200 °C, from -1069 to -951 J/mol at 220 °C, and from -911 to -793 J/mol at 250 °C, respectively. Therefore, the phase transformation of undercooled austenite is curbed with Ni addition.

In addition, it can be observed from Table 2 and Fig. 3 that when the samples of same steel (Ni-free or Ni-added steel) are austempered at different temperatures from 200 to 250 °C, the bainite amount first increases and then decreases with the increase of the austempering temperature. It is inconsistent with the result reported by Caballero et al. [1]. They stated that the amount of bainite ferrite decreased with the increase of transformation temperature. It may be ascribed to the different chemical composition and transformation time in two studies, fourteen days of transformation time and the chemical composition of 0.79C-1.59Si-1.94Mn-1.33Cr-0.30Mo-0.11V (wt%) in their study, but 30 h of transformation time and the chemical composition of 0.80C-1.60Si-2.00Mn-1.00Cr-0.30Mo-1.50Co-1.0Al or 0.80C-1.60Si-2.00Mn-1.00Cr-0.30Mo-1.00Ni-1.50Co-1.00Al (wt%) in the present study. In the present study, the sample austempered at a medium temperature (220 °C) obtains the largest bainite amount. The result may be attributed to the combination effect of the driving force for transformation and the capability of atomic diffusion.

The relationship between the diffusion coefficient of carbon atoms and temperature is given in Eq. (2) [23].

$$D = D_0 \exp(-Q_i/RT) \quad (2)$$

where D and D_0 are the diffusion coefficient and the diffusion constant of carbon in austenite, respectively. R represents the gas constant and T is the temperature. Q_i is the activation energy representing the barrier to transfer atoms across the interface. It indicates that the diffusion capability of carbon atoms increases with the temperature, while the driving force for transformation decreases with the increase of temperature (Fig. 4b). When the sample is transformed at higher temperature, the capability of atomic diffusion is larger, whereas the driving force for transformation is

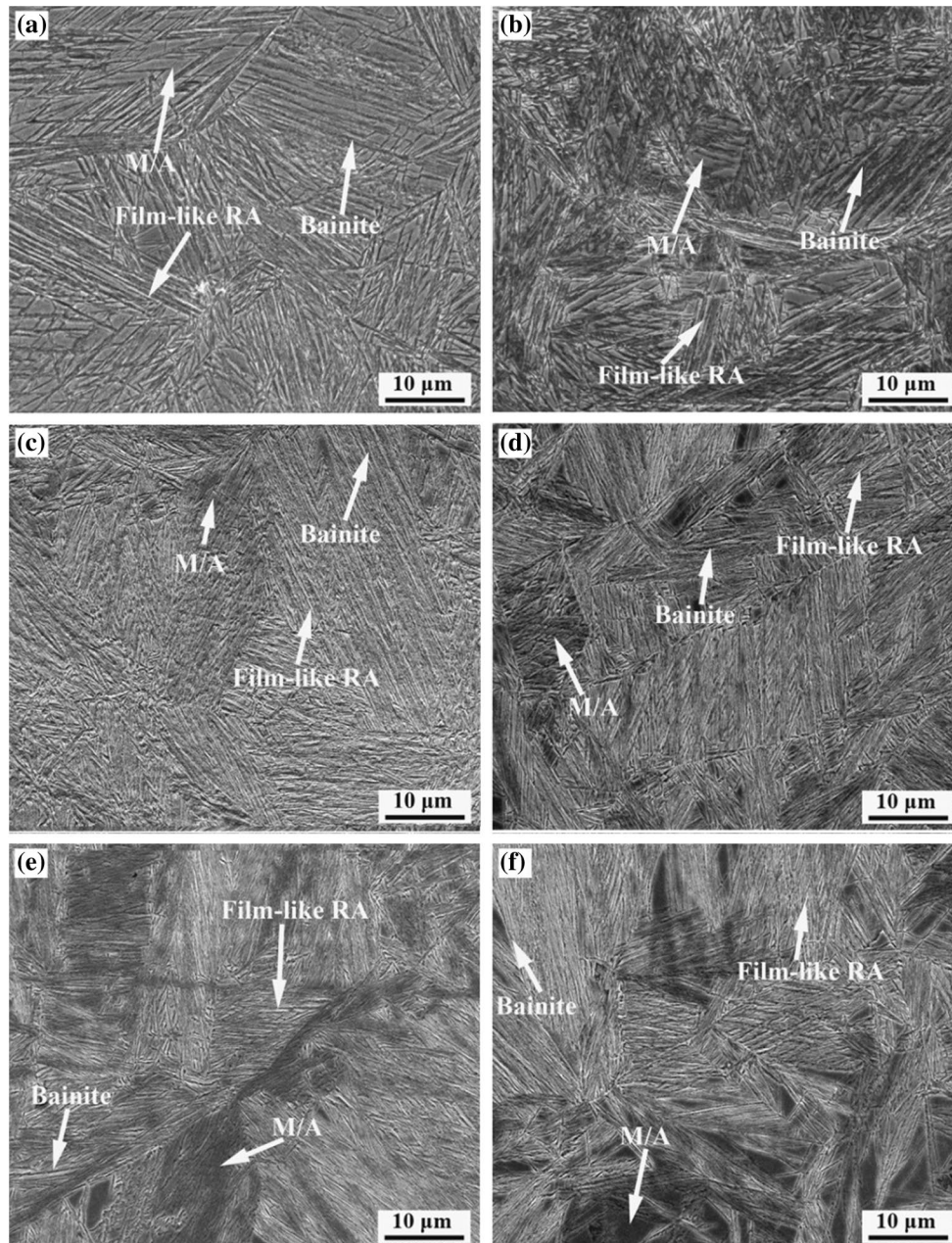


Fig. 3 The microstructure of different samples austempered at different temperatures for 30 h: **a** Ni-free steel, 200 °C; **b** Ni-added steel, 200 °C; **c** Ni-free steel, 220 °C; **d** Ni-added steel, 220 °C; **e** Ni-free steel, 250 °C; **f** Ni-added steel, 250 °C

Table 2 The volume fractions of bainite and RA

Treatments	Steels	$V_{(B)}$ (%)	$V_{(RA)}$ (%)
200 °C for 30 h	Ni-free	32.64 ± 3.03	22.59 ± 3.80
	Ni-added	30.85 ± 2.07	20.60 ± 4.56
220 °C for 30 h	Ni-free	57.67 ± 1.69	37.32 ± 1.44
	Ni-added	52.18 ± 2.43	28.66 ± 6.73
250 °C for 30 h	Ni-free	44.87 ± 1.23	29.21 ± 6.43
	Ni-added	36.89 ± 2.12	23.97 ± 2.11

$V_{(B)}$ and $V_{(RA)}$, the volume fractions of bainite and RA

small. On the contrary, when the sample is transformed at lower temperature, the driving force for transformation is larger, whereas the capability of atomic diffusion is weak. Moreover, the transformation time for finishing bainite transformation is as long as several days or longer due to the high carbon content. In order to balance the product costs and mechanical property in practical industrial production, the transformation time of 30 h is selected in the present study. The tendency of bainite amount with temperature is schematically shown in diagram Fig. 5. In the given

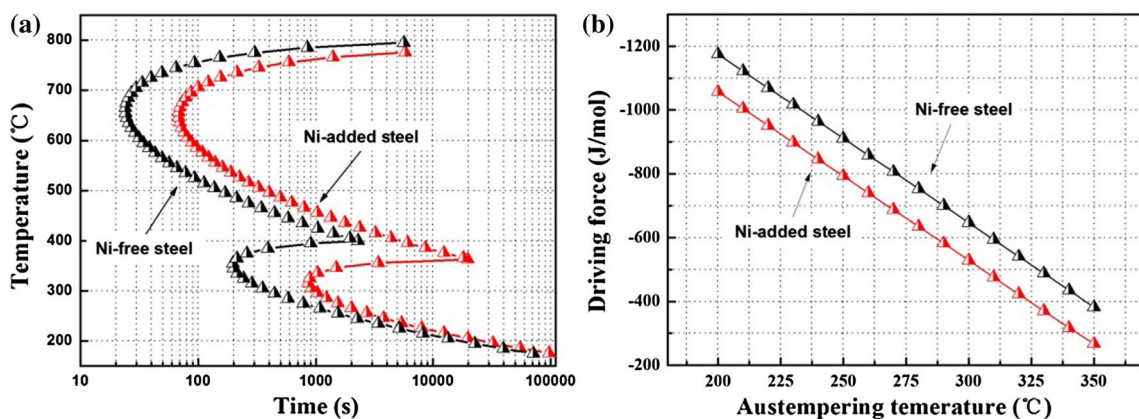


Fig. 4 a The time–temperature–transformation (TTT) curves and b the values of $\Delta G^{\gamma \rightarrow \alpha}$ versus temperature of two steels

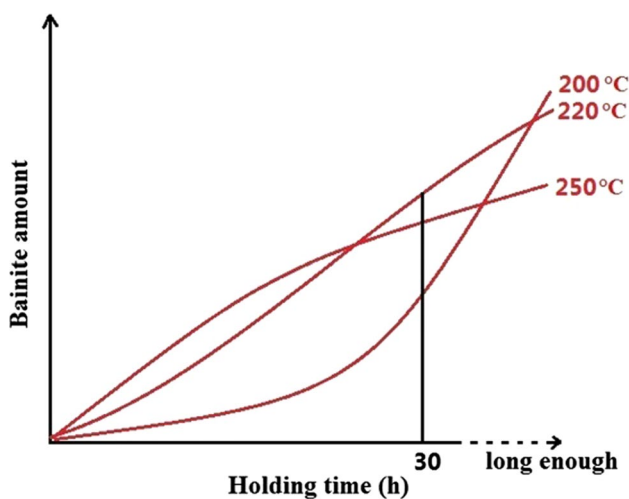


Fig. 5 The variation tendency of bainite amount versus holding time

transformation time of 30 h, the samples of Ni-free steel or Ni-added steel austempered at medium temperature of 220 °C both obtain the largest bainite amount.

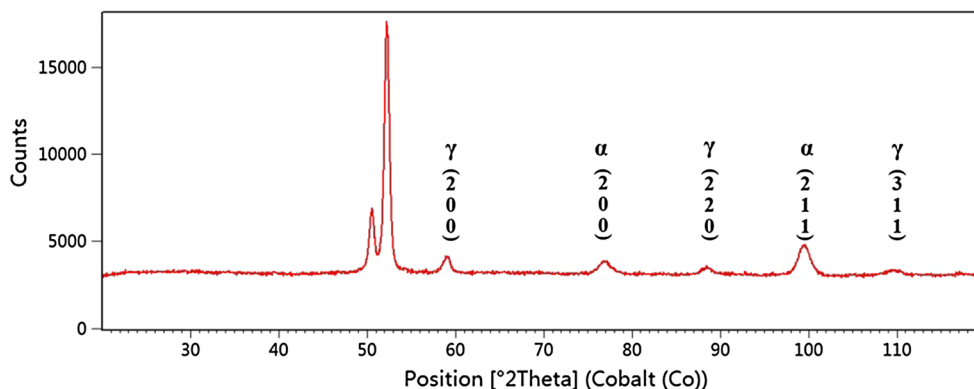
3.1.2 XRD Characteristic

Figure 6 presents an example of XRD diffraction pattern of Ni-free steel transformed at 200 °C for 30 h. According to the integrated intensities and the angles of diffraction peaks, the RA volume fractions in different samples were calculated using the method described in Ref. [24]. The RA volume fractions were calculated by the integrated intensities of (200) α , (211) α , (200) γ , (220) γ and (311) γ diffraction peaks according to Eq. (2) [24].

$$V_i = \frac{1}{1 + G(I_\alpha/I_\gamma)} \tag{2}$$

where V_i presents the volume fraction of austenite for each peak; I_α and I_γ present the corresponding integrated intensities of ferrite and austenite; G is the ratio of the intensity factor corresponding to the austenite crystal face (hkl) $_j$ and the martensite crystal face (hkl) $_i$, and its value is 2.5 for $I_\alpha(200)/I_\gamma(200)$, 1.38 for $I_\alpha(200)/I_\gamma(220)$, 1.78 for $I_\alpha(200)/I_\gamma(311)$, 1.19 for $I_\alpha(211)/I_\gamma(200)$, 0.06 for $I_\alpha(211)/I_\gamma(220)$, 0.87 for $I_\alpha(211)/I_\gamma(311)$, respectively. The calculated results are given in Table 2. It indicates that for

Fig. 6 An example of XRD diffraction pattern of Ni-free steel transformed at 200 °C for 30 h



the same heat treatment, the addition of Ni results in the decrease of volume fraction of RA. Moreover, for the same steel, the amount of RA increases firstly and then decreases with temperature. The RA volume fraction is determined by the volume fraction of bainite and martensite. It is known that a larger fraction of bainite favors the retention of austenite because the partitioning of abundant carbon into the austenite retards the formation of martensite after isothermal transformation [25, 26]. Therefore, the more RA is retained due to more volume of bainite.

3.1.3 Mechanical Properties

The tensile results of Ni-free steel and Ni-added steel treated by different treatments are given in Table 3 and plotted in Fig. 7. When the austempering temperature is 200 °C, the Ni-added steel showed a slight increase in yield strength (YS) and total elongation (TE), whereas the tensile strength (TS) decreases marginally compared with that of the Ni-free steel. As a result, the product of tensile strength and elongation (PSE) doesn't show an obvious increment with Ni addition. It indicates that the effect of Ni addition on mechanical property is very small at the austempering temperature of 200 °C. When the austempering temperatures are 220 and

Table 3 The tensile results of two tested steels by the different heat treatments

Treatment	Steels	YS (MPa)	TS (MPa)	TE (%)	PSE (GPa%)
200 °C for 30 h	Ni-free	1053 ± 36	1436 ± 54	5.6 ± 0.3	8.04 ± 0.79
	Ni-added	1084 ± 27	1383 ± 46	6.1 ± 0.4	8.43 ± 0.52
220 °C for 30 h	Ni-free	1767 ± 37	1971 ± 26	10.4 ± 0.6	20.51 ± 0.98
	Ni-added	1441 ± 42	1792 ± 34	9.8 ± 0.2	17.02 ± 0.76
250 °C for 30 h	Ni-free	1610 ± 26	1912 ± 31	10.1 ± 0.5	19.31 ± 0.45
	Ni-added	1558 ± 37	1725 ± 45	8.9 ± 0.4	15.35 ± 0.63

YS yield strength, TS tensile strength, TE total elongation

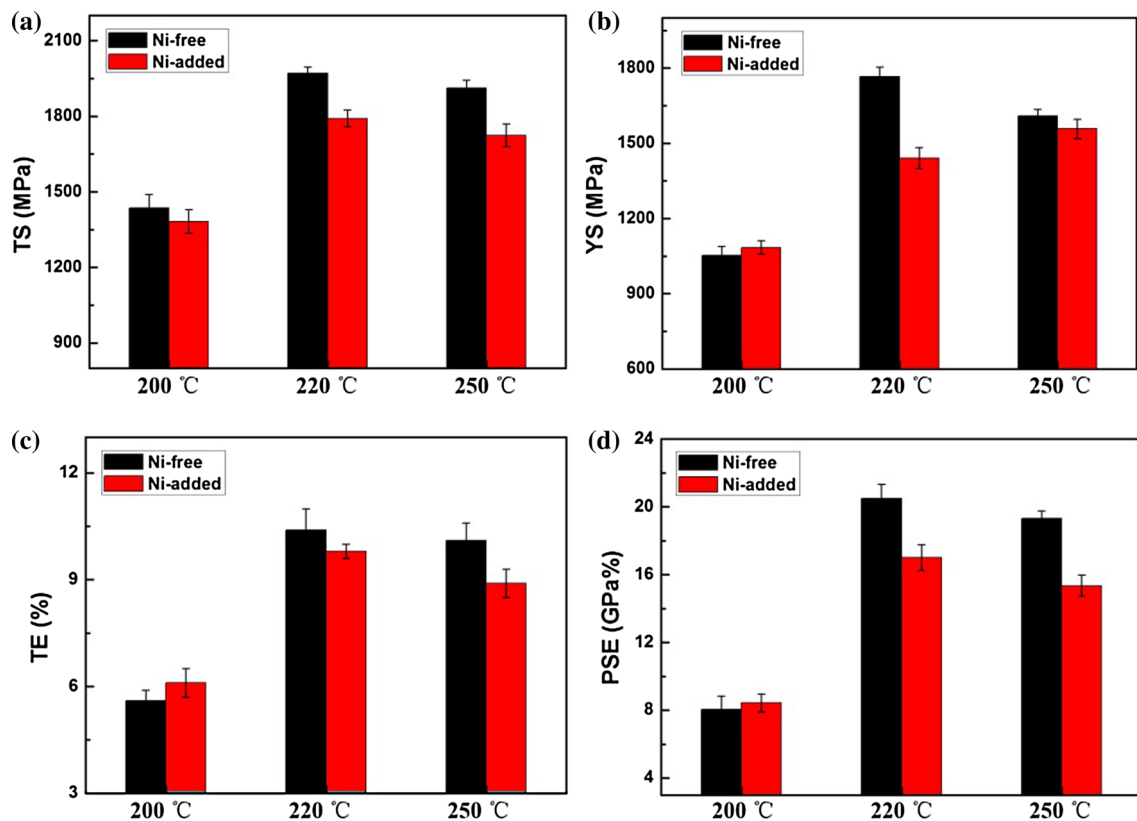


Fig. 7 Comprehensive properties of two steels treated by different processes

250 °C, the TS, YS and TE all decrease with Ni addition, resulting in an obviously decline in PSE compared to that of the Ni-free steel. The main reason is that Ni addition retards the bainite transformation and the hindrance of Ni on bainitic transformation is more obvious at higher transformation temperatures. From Fig. 4b, it can be observed that the driving forces for bainite transformation with Ni addition decrease 11.16% at 200 °C, 12.41% at 220 °C, and 14.88% at 250 °C, respectively, indicating that the decrease of driving force accounts for a larger proportion at the higher transformation temperature. Consequently, the decrease of bainite amount with Ni addition is more obvious at austempering temperatures of 220 and 250 °C. At higher austempering temperature, less bainite amount with Ni addition leads to more undecomposed austenite to transform into blocky M/A in Ni-added steel, as shown in Fig. 3. The blocky M/A is a brittle phase and is very unstable when loaded [27]. It intensively deteriorates the comprehensive properties of bainitic steels. Moreover, the more bainite plates can distinctly increase the strength and elongation of bainitic steels due to the grain refining strengthening. It is well known that in high carbon bainitic steel, more volume of ultrafine bainite plates means better mechanical properties [28, 29]. Furthermore, Ni addition lowers the amount of film-like RA. The film-like RA can bring a significant increment in mechanical property by the effect of TRIP (transformation induced plasticity) [30, 31]. Therefore, the mechanical property of high carbon bainitic steel becomes worse with Ni addition at higher austempering temperature, and it shows no significant difference at lower austempering temperature. It might be deduced that if only considering the mechanical property of high carbon bainitic steels, the addition of Ni may be avoided during the isothermal bainite transformation.

The present result is different with the result reported by Chen et al. [12]. In their study, Ni addition resulted in better mechanical property of a bainitic steel. The difference may be attributed to the different heat treatment procedures, i.e., the continuous cooling in their study and the isothermal holding in the present study. During continuous cooling process, Ni addition increases the stability of austenite, and obviously delays ferrite transformation, so it results in the formation of more volume fraction of bainite. Thus, it can be inferred that Ni addition does not promote bainite transformation by itself, but the promotion mainly results from the inhibition of Ni on ferritic transformation. In austempering process, no ferrite appears even in the Ni-free steel due to the quick cooling rate before austempering. Compared to Ni-free steel, there is less bainite amount in Ni-added steel because of the decrease of the driving force for bainite transformation with Ni addition (Table 2). Less volume of bainite leads to the lower mechanical properties in high carbon bainitic steels. Therefore, Ni addition results in the better mechanical properties in their study, but it leads

to the decrease of mechanical properties in present study. It is reasonable to conclude that the effect of Ni on property of high strength bainitic steels depends on heat treatment procedure.

In addition, for the same steel (Ni-free or Ni-added steel), the largest bainite and RA amount are obtained at the medium austempering temperature (Table 2), so the highest PSE is obtained when the samples are austempered at the medium austempering temperature.

3.2 Effect of Austempering Time

3.2.1 Microstructure and XRD Result

The SEM microstructures of Ni-free steel austempered at 220 °C for different times of 15, 25 and 30 h are presented in Fig. 8. The samples held for 15 and 25 h mainly consist of lath-like bainite, blocky M/A and film-like RA, whereas few M/A appears in the sample held for 30 h. It indicates that the amount of M/A decreases with the increase of transformation time. Similarly, the volume fraction of bainite in different samples was calculated by the Image-Pro Plus software using the same method proposed in Sect. 3.1.1. The volume fractions of bainite are 37.13% for 15 h, 52.18% for 25 h, and 57.67% for 30 h, respectively. It indicates that the amount of bainite transformation gradually increases with the transformation time.

Figure 9 shows the curves of the volume fraction of bainite versus holding time during isothermal transformation. It can be observed that there is no apparent smooth and near-horizontal stage before 30 h, so it can be inferred that the bainite transformation doesn't stop even the transformation time is as long as 30 h.

The volume fractions of RA of different samples were also measured by the XRD tests. For different samples transformed at 220 °C, they are 28.65% for 15 h, 34.13% for 25 h, and 37.75% for 30 h, respectively. It indicates that the volume fraction of RA increases with prolonging the isothermal transformation time. It is because the formation of more bainite ejects abundant carbon into undecomposed austenite, which results in less austenite to transform into blocky M/A due to higher stability of austenite, so more volume of RA is retained at room temperature with the prolongation of transformation time.

3.2.2 Mechanical Properties

Table 4 shows the tensile results of different samples austempered at 220 °C for different holding times. The sample transformed for 30 h achieves the largest strength of 1971 MPa and the best total elongation of 10.4%. So the highest PSE of 20.51 GPa % can be obtained by prolonging the transformation time to 30 h. It means that when

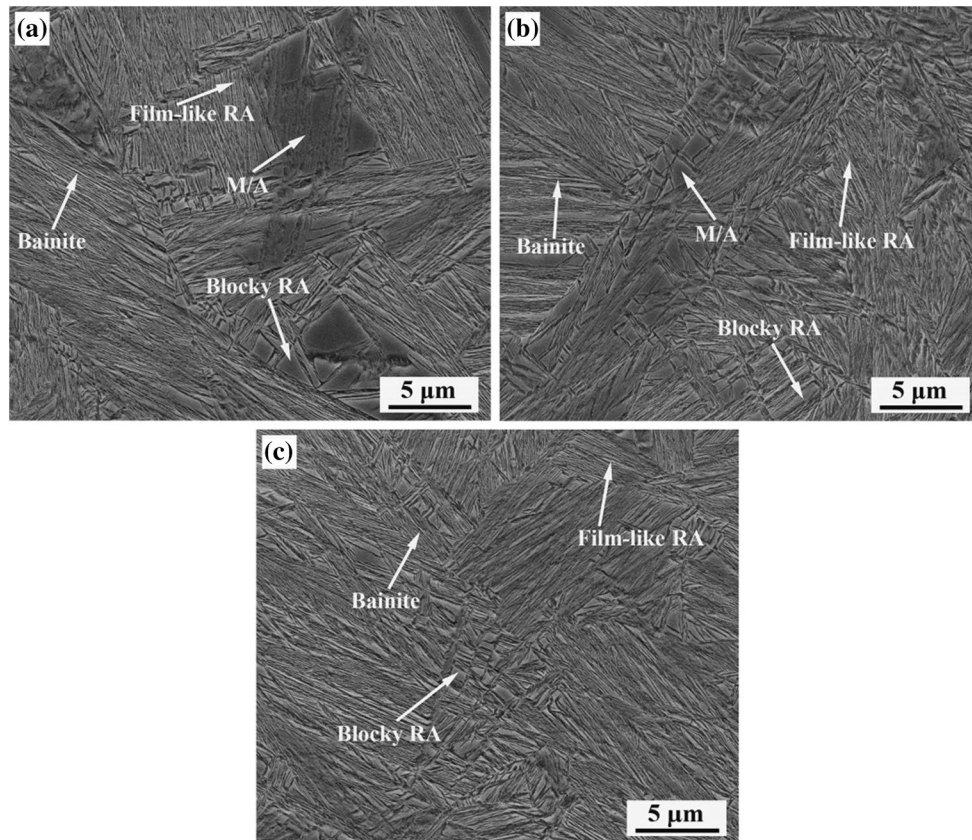


Fig. 8 The SEM microstructure of Ni-free steel austempered at 220 °C for: a 15 h, b 25 h, and c 30 h

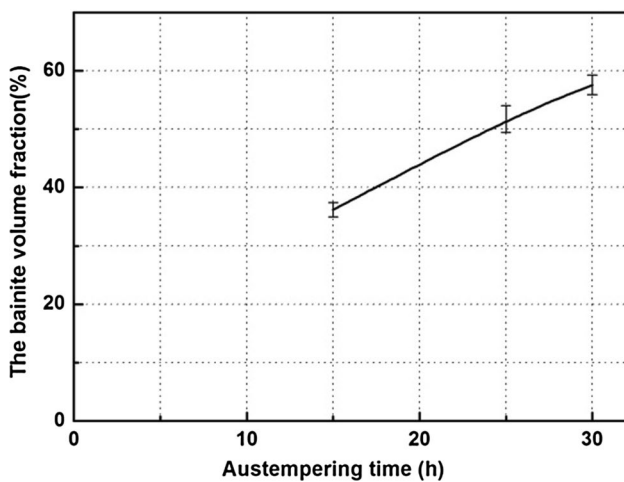


Fig. 9 The curves of the volume fraction of bainite versus austempering time

the samples are austempered at 220 °C and in a given transformation time range of 30 h, an increase in the isothermal transformation time can result in better mechanical properties. After isothermal bainite transformation, the undecomposed austenite is reserved as M/A and RA at

Table 4 The tensile results of Ni-free steel treated by different transformation times

Treatment	YS (MPa)	TS (MPa)	TE (%)	PSE (GPa%)
220 °C for 15 h	1269 ± 23	1647 ± 36	7.5 ± 0.4	12.35 ± 0.79
220 °C for 25 h	1679 ± 11	1932 ± 14	8.7 ± 0.3	16.81 ± 0.55
220 °C for 30 h	1767 ± 37	1971 ± 26	10.4 ± 0.6	20.51 ± 0.98

room temperature. The increase of bainite amount brings a decrease in the amount of blocky M/A and an increase in the amount of film-like RA by prolonging the holding time. The blocky M/A is unstable when subjected to external loads. Moreover, the blocky M/A is considered to be a brittle phase and it deteriorates the strength and ductility of the steels. When the transformation time is short, there is still large amount of undecomposed austenite preserved as the blocky M/A due to the lower carbon content in undecomposed austenite. With the increase of transformation time, the amount of bainite increases, so the amount of blocky M/A decreases and the amount film-like RA, which is distributed between the bainite plates, increases. The film-like RA has higher stability and the mechanical properties is improved by the TRIP effect [30, 31]. In

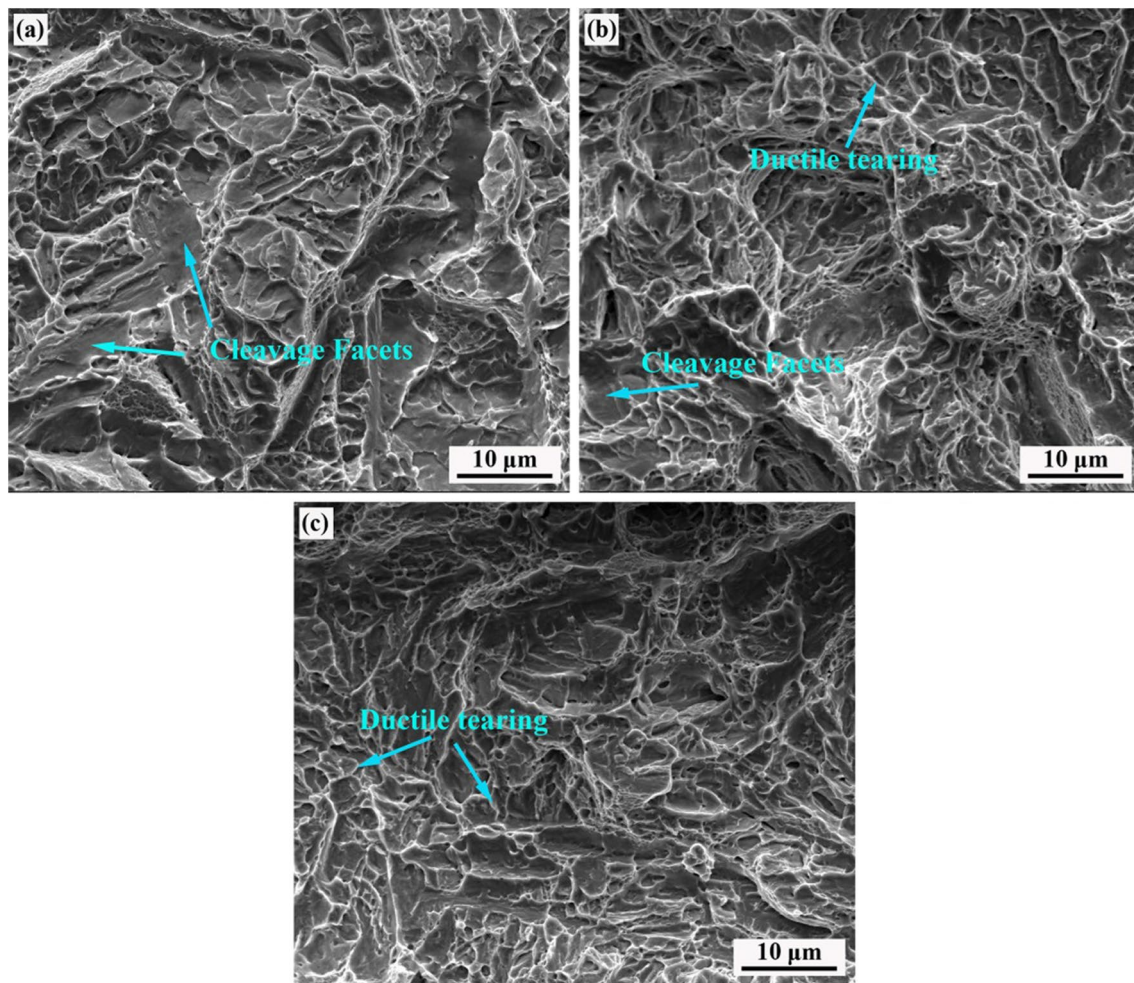


Fig. 10 SEM micrographs of fracture surface for the samples austempered at 220 °C for: **a** 15 h, **b** 25 h, and **c** 30 h

addition, the more bainite plates mean the better mechanical properties in high carbon bainitic steels. Therefore, when the samples are austempered at 220 °C, in a given transformation time range in present study, the prolongation of the isothermal transformation time improves the comprehensive properties of high carbon bainitic steels.

Figure 10 shows the SEM micrographs of the fracture surface of different tensile specimens. The fracture of different specimens mainly consists of cleavage facet and ductile tearing. Ductile tearing is regarded as a feature of the ductile fracture mode, which implies high tensile toughness. On the contrary, cleavage facet represents the feature of brittle fracture, which expresses the inferior tensile toughness [32]. The fracture surface of specimen held for 15 h contains a lot of cleavage facets, whereas more volume of ductile tearing morphology appears in the specimen held for 30 h, indicating that the tensile toughness increases with prolonging the holding time. It is consistent with the result in Table 4.

4 Conclusions

Two high carbon ultrahigh strength bainitic steels and multiple austempering processes were designed to investigate the effects of Ni addition and holding time on bainite transformation and properties using metallographic, X-ray diffraction and tensile test. The conclusions can be drawn as follows:

1. The addition of Ni retards the kinetics of isothermal bainite transformation and decreases the amount of isothermal bainite transformation due to the decrease in chemical driving force for nucleation and growth of bainite.
2. The mechanical property of high carbon bainitic steels decreases with Ni addition at higher austempering temperature, and it shows no significant difference at lower austempering temperature.

3. For the same steel, the amounts of bainite and RA firstly increase and then decrease with the increase of the austempering temperature. As a result, the sample transformed at medium austempering temperature (220 °C) obtains better comprehensive property.
4. In the given transformation time range of 30 h, the extension of transformation time is favorable for obtaining better mechanical properties.

Acknowledgements The authors gratefully acknowledge the financial supports from the Major Projects of Technological Innovation in Hubei (No. 2017AAA116), the National Natural Science Foundation of China (No. 51274154) and the National Nature Science Foundation of China (No. 51704217).

References

1. F.G. Caballero, H.K.D.H. Bhadeshia, *Curr. Opin. Solid State Mater. Sci.* **8**, 251 (2004)
2. J. Zhao, J.M. Li, H.H. Ji, T.S. Wang, *Materials* **10**, 874 (2017)
3. L.X. Li, L.Y. Zheng, B. Ye, Z.Q. Tong, *Met. Mater. Int.* **24**, 60 (2018)
4. C. Garcia-mateo, F.G. Caballero, H.K.D.H. Bhadeshia, *ISIJ Int.* **43**, 285 (2003)
5. F.G. Caballero, H.K.D.H. Bhadeshia, K.J.A. Mawella, D.G. Jones, P. Brown, *Mater. Sci. Technol.* **18**, 279 (2002)
6. J.Y. Tian, G. Xu, M.X. Zhou, H.J. Hu, X.L. Wan, *Metals* **7**, 40 (2017)
7. H.J. Hu, G. Xu, M.X. Zhou, Q. Yuan, *Metals* **6**, 173 (2016)
8. E. Keehan, L. Karlsson, H.O. Andrén, H.K.D.H. Bhadeshia, *Weld. J.* **85**, 200 (2006)
9. E. Keehan, H.O. Andrén, L. Karlsson, M. Murugananth, H.K.D.H. Bhadeshia, in *6th International Conference on Trends in Welding Research*, ed. by S.A. David, T. DebRoy, J.C. Lippold (ASM International, Phoenix, 2002), p. 695
10. J.A. Omotoyinbo, O.O. Oluwole, *Mater. Des.* **30**, 335 (2009)
11. S. Zhang, P. Wang, D. Li, Y. Li, *Mater. Des.* **84**, 385 (2015)
12. Y.L. Chen, C.Z. Dong, Q.W. Cai, D.C. Wan, L. Li, Y. Qi, *J. Mater. Eng.* **3**, 16 (2013)
13. X.Y. Long, F.C. Zhang, J. Kang, B. Lv, X.B. Shi, *Mater. Sci. Eng. A* **594**, 344 (2014)
14. J. Kobayashi, D. Ina, N. Yoshikawa, S. Koh-Ichi, *ISIJ Int.* **52**, 1894 (2012)
15. L.C. Chang, *Metall. Mater. Trans. A* **30**, 909 (1999)
16. L.H. Qian, Q. Zhou, F.C. Zhang, J.Y. Meng, M. Zhang, Y. Tian, *Mater. Des.* **39**, 264 (2012)
17. F. Hu, K.M. Wu, H. Zheng, *Steel Res. Int.* **84**, 1060 (2013)
18. M.X. Zhou, G. Xu, L. Wang, H.J. Hu, *Trans. Indian Inst. Met.* **69**, 693 (2016)
19. S. Baradari, M.A. Boutorabi, *Mater. Des.* **86**, 603 (2015)
20. M.X. Zhou, G. Xu, J.Y. Tian, H.J. Hu, Q. Yuan, *Metals* **7**, 263 (2017)
21. J.Y. Tian, G. Xu, M.X. Zhou, H.J. Hu, *Steel Res. Int.* (2018). <https://doi.org/10.1002/srin.201700469>
22. M.X. Zhou, G. Xu, H.J. Hu, Q. Yuan, J.Y. Tian, *Steel Res. Int.* (2016). <https://doi.org/10.1002/srin.201600377>
23. B. Ozturk, V.L. Fearing, J.A. Ruth, G. Simkovich, *Solid State Ionics* **12**, 145 (1984)
24. C.Y. Wang, J. Shi, W.Q. Cao, H. Dong, *Mater. Sci. Eng. A* **527**, 3442 (2010)
25. D. Quidort, Y. Bréchet, *Scripta Mater.* **47**, 151 (2002)
26. J.Y. Tian, G. Xu, L. Wang, M.X. Zhou, H.J. Hu, *Trans. Indian Inst. Met.* **71**, 185 (2018)
27. H.J. Hu, G. Xu, L. Wang, M.X. Zhou, Z.L. Xue, *Met. Mater. Int.* **21**, 929 (2015)
28. C. Garcia-Mateo, M. Peet, F.G. Caballero, H.K.D.H. Bhadeshia, *Mater. Sci. Technol.* **20**, 814 (2014)
29. C. Garcia-Mateo, F.G. Caballero, *Mater. Trans.* **46**, 1839 (2005)
30. B.C.D. Cooman, *Curr. Opin. Solid State Mater. Sci.* **8**, 285 (2004)
31. M. Pozuelo, J.E. Wittig, J.A. Jiménez, G. Frommeyer, *Metal. Mater. Trans. A* **40**, 1826 (2009)
32. G. Mandal, C. Roy, S.K. Ghosh, S. Chatterjee, *J. Alloys Compd.* **705**, 817 (2017)